EPSC2018

EXO5 abstracts

EPSC Abstracts
Vol. 12, EPSC2018-19, 2018
European Planetary Science Congress 2018

On localization of exoplanets radiation belts

Nikolay Perov (1, 2), Anar Abduragimov (2)
(1) Cultural and Educational Centre named after V.V. Tereshkova, Yaroslavl, Russian Federation
(2) State Pedagogical University named after K.D. Ushinskii, Yaroslavl, Russian Federation (perov@yarplaneta.ru / Fax: +7 (4852) 72-63-90)

1. Introduction

In present time there are known about 2000 exoplanetary systems and 4000 exoplanets. Discovering of the first exoplanets since 1995 found the significant distinguishes theirs dynamical, physical and chemical properties in comparison with properties of the Solar system planets. But modern investigations [1] show the existence of the exoplanetary systems and exoplanets with properties characteristically for the Solar system and the Solar system planets. For example, in Fig.1 and Fig.2, in according with the work [1], the distributions "Planet Semi-Major Axis vs Planet Radius" are plotted for data of 2011 and 2016, correspondingly. These figures allow making a conclusion – the number of the revealed exoplanets with small radii near the parent stars is increasing and the number of giant planets placed far from the stars is also increasing. In the work [2] results are discussed of research on magnetospheres of Jupiter, Saturn, Uranus, Neptune and the Earth. Below we consider a method of finding in the space-time of undiscovered exoplanets radiation belts.

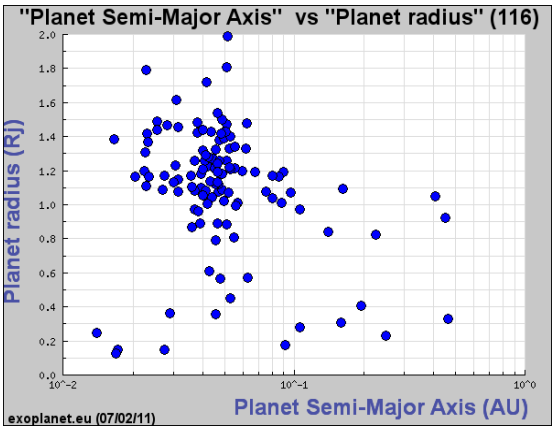

Figure 1: Distribution of exoplanets in 2011 – "Radius-Semi Major Axis" [1].

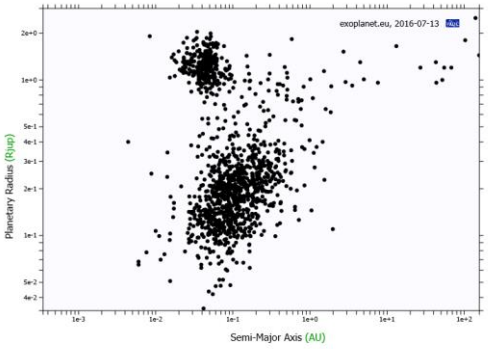

Figure 2: Distribution of exoplanets in 2016 – "Radius-Semi Major Axis" [1].

2. The peculiarities of perturbations of semi-major axes of small bodies moved in magnetic and gravitational fields of rotating exoplanet

Let us consider action of dipole magnetic field of a rotating planet, with mass M and angular velocity w, on a body with mass m and electric charge Q in the frame of the model described by the equation (1)

$$d^2\mathbf{r}/dt^2=-G(M+m)\mathbf{r}/r^3+Q/m[\mathbf{V},\mu_0\mathbf{H}]. \quad (1)$$

Here, $\mathbf{r}$ is the planet centric radius vector of the satellite, GM is the planet centric gravitational constant, μ_0 is the magnetic constant, $\mathbf{V}$ is the velocity of the satellite in the magnetic field of the planet, $\mathbf{H}$ is the intensity of planet magnetic field. We use the following conditions

$$M>>m;G(M+m)>>|Q/m[\mathbf{V},\mu_0\mathbf{H}], \mathbf{V}=\mathbf{v}-\mathbf{V}_M, e^2\approx 0. \quad (2)$$

$\mathbf{v}$ is the velocity of the satellite in respect of the inertial system of origin, $\mathbf{V}_M$ is the velocity of the point hardly tied with the rotating planet.

Components of the magnetic intensity $\boldsymbol{H}$ are depended on the coordinates and may be determined from the expression of the "potential" U of the magnetic field [4]

$$U=R^3/r^2[g_1^0 sin\varphi+(g_1^0 cos\lambda+h_1^1 sin\lambda)cos\varphi]. \quad (3)$$

Where R is the equatorial radius of the planet, φ and λ are the "planet graphic" latitude and longitude of the projection of the satellite on the surface of the planet. For the Earth, as it is known, g_1^0=-30186γ; g_1^1=-2036γ; h_1^1=+5735γ. $1\gamma = 10^{-2}/(4\pi)A/m = 7.95775\cdot10^{-4}$ A/m [4].
If X, Y, Y are the northern, eastern and vertical components of the vector $\boldsymbol{H}$, correspondingly, then

$$X=-1/r(\partial U/\partial\varphi);\ Y=-1/(rcos\varphi)(\partial U/\partial\lambda);\ Z=-\partial U/\partial r. \quad (4)$$

Using the Lagrange equations for the calculations of perturbations of semi major axis δa per one revolution of the satellite with mean motion equals n_s [3] and equation (1) – (4) we obtained the following results, for example

if $w/n_s=2\pm\varepsilon$; $\varepsilon\rightarrow 0$, than

$$\delta a=2\pi(Q/m)R^3\mu_0 wa/(GM)sini\cdot\{(g_1^1 cos\lambda_{\Omega 0}+h_1^1 sin\ \lambda_{\Omega 0})\cdot(cos2\omega+sin2\omega)+cosi\cdot[(g_1^1 sin\lambda_{\Omega 0}-h_1^1 cos\lambda_{\Omega 0})\cdot sin2\omega + (-g_1^1 cos\lambda_{\Omega 0}+h_1^1 sin\ \lambda_{\Omega 0})\cdot cos2\omega]\}, \quad (5)$$

where e and i, are the eccentricity of the orbit, the inclination of the orbital plane, correspondingly, ω is the argument of the percenter of the satellite orbit, $\lambda_{\Omega 0}$ is initial planet graphic (Greenwich for the Earth) longitude of the satellite. It should be noted the explicit formula for δa is very complicated (even for the conditions (2)), but this expression is significantly simplified for the ratios w/n_s=1, 2, 3… . It is obviously, for the definite values of the parameters, placed in the equation (5), we have δa=0.

3. (Any) regions with radiation belts near the planets

So, in the case of the planet dipole magnetic field it may be shown the expressions for the perturbations of semi-major axes δa of the satellites orbits are presented in the "simple" forms for a for which periods of the satellites motion are multiples of the axial rotating planet period T (4) (in the frame of the considered model).

$$a=\left(\frac{\left(\frac{T}{n}\right)^2 GM}{4\pi^2}\right)^{1/3}. \quad (4)$$

Here, G is the gravitational constant; M is the planet's mass. For the Earth radiations belts ½<n<9 (the Earth radiation belts are placed from the planet at the distances equal 3000 - 12000 km, 18000 - 57000 km, the third belt is placed from the planet at the distance equal the ten radii of the Earth but this is unstable region of charged particles motion [2, 4]). In the case of Jupiter the maximum charged particles concentration is placed at the distance equals 177000 km [2], corresponding a for ½<n<4 (4). Suppose, exosolar planets, especially rotating with great angular velocities, have radiation belts placed in the regions determined by the formula (4).

4. Conclusions

Discovering of the general properties of exoplanets and Solar system planets, give possibilities to localize unrevealed yet small bodies near the exosolar planets. For instance, the formula (4), in the considered model, allows to estimate the size r of the regions with hypothetical planets radiation belts (1/2<n<10, r>R, T≤1 day).

References

[1] http://nssdc.gsfc.nasa.gov/planetary/

[2] van Allen and James A.: Why radiation belts exist, Iowa, University, Iowa City, Earth in Space, vol. 4, Oct, 1991, pp.5–7.

[3] King-Hele, D.: Theory of satellite orbits in an atmosphere, Butterworths London, 1964, 165 pp.

[4] Yanovskii, B.M.: The terrestrial magnetism, Leningrad, Leningrad State University, 1978, 592 pp.

EPSC Abstracts
Vol. 12, EPSC2018-126, 2018
European Planetary Science Congress 2018

Stellar wind interaction with the expanding atmosphere of Gliese 436b

A.G. Berezutskiy (1), I.F. Shaikhislamov (1), M.L. Khodachenko (2,3) and I.B. Miroshnichenko (1,4)
(1) Institute of Laser Physics, Siberian Brunch Russian Academy of Science, Novosibirsk, Russia;
(2) Space Research Institute, Austrian Academy of Science, Graz, Austria;
(3) Skobeltsyn Institute of Nuclear Physics, Moscow State University, Moscow, Russia
(4) Novosibirsk State Technical University, Novosibirsk, Russia
(a.berezuckiy@yandex.ru)

Abstract

We study an exosphere of a Neptune-size exoplanet Gliese 436b, orbiting the red dwarf at an extremely close distance (0.028 au), taking into account its interaction with the stellar wind plasma flow. It was shown that Gliese 436 b has a bowshock region between planetary and stellar wind which localized on the distance of ~33 R_p, where density of planetary atoms slightly dominates over the protons.

1. Introduction

The modelled planet Gliese 436b has a mass $M_p=0.07M_J$, radius $R=0.38R_J$ and an estimated surface temperature 700 K. To describe the physical processes in the planetary upper atmosphere and beyond, we use a 2D self-consistent multi-fluid hydrodynamic 2D aeronomy model. In our simulations we investigated basic properties of exosphere during interaction with stellar plasma.

2. Model

To describe the expanding atmosphere of Gliese 436b and its interaction with the stellar wind plasma, we use a 2D axisymmetric multi-fluid hydrodynamic model [1, 2]. Each fluid describes the hydrogen and helium components of the planetary origin (H, H^+, H_2, H_2^+, H_3^+, He, He^+) and the stellar wind protons. The planetary plasma is regarded as a quasineutral fluid with thermal equilibrium: $T_i = T_e$. The model takes into account the basic photo-chemical processes in the hydrogen-dominated atmosphere, allowing to describe in a self-consistent way its heating and ionization due to absorption of the stellar XUV radiation. An approximated spectrum of Gliese 436 in the range of 10-912 Å is used in the simulations. The tidal forces acting on the streams of the escaping planetary upper atmospheric material are also taken into account.

3. Results

At the initial state of the simulations, the atmosphere of Gliese 436b is assumed to consist of the molecular hydrogen and helium atoms at a ratio $N_{He} / N_{H2} = 1/5$ with the temperature 750 K. We consider the case of a weak stellar wind (SW) with $n_{sw}=100$ cm^{-3}, $T_{sw}=1$ MK, $V_{sw}=70$ km/s, which is much less intense than the solar wind. Because of this fact, , we did not consider generation of Energetic Neutral Atoms (ENAs). The planetary wind (PW) streams, moving towards and away from the star, are formed, driven by the stellar XUV energy input and the stellar gravity. They propagate within the SW plasma, separated from it by a kind of ionopause. In our simulations we took the stellar XUV flux F_{XUV}= 0.8 erg cm^{-2}s^{-1}at a distance of 1 a.u.

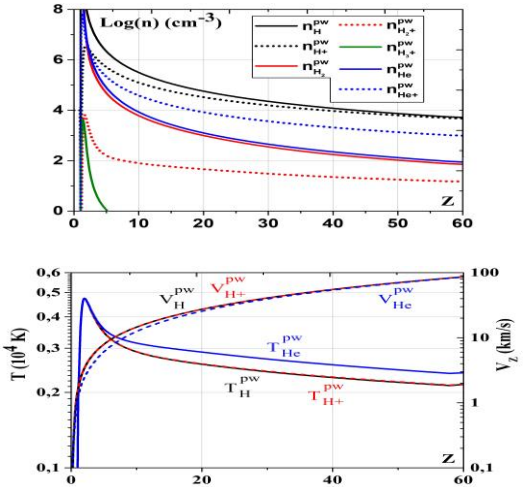

Fig.1 Distribution of density, temperature and velocity of the species in the PW along the planet-star line.

The structure of the expanding PW of Gliese 436 b is shown in Figure 1, which gives the profiles of density, velocity, and temperature for hydrogen atoms, protons and helium atoms along the planet-star line. A strong coupling between atoms and protons in the PW region is indicated by the velocity and temperature profiles, which are rather close to each other. The velocity rapidly increases and at the distance of 50-60 R_p from the planet it reaches ~90 km/s, while the temperature after having a maximum of about 5000 K decreases smoothly down to ~ 2200 K.

The distributions of density and velocity of the species in the PW cross the planet-star line is shown in Figure 2, which reveals three regions: 1) the region of the PW material; 2) an outside area of the SW; and 3) a bowshock between the PW and SW where density and the temperature of the planetary atoms and protons increase. The density of planetary atoms slightly dominates over the protons in the region of the bowshock. Planetary atoms, overcoming the shock, also penetrate into the SW, where they are accelerated up to speeds of ~ 30 km/s, at the distance of ~60Rp, while the planetary protons are stopped by the thermal pressure of the stellar wind protons. PW atoms which penetrate into SW undergo the charge exchange with stellar protons forming ENAs.

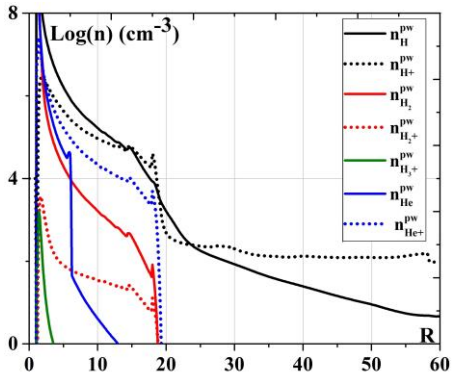

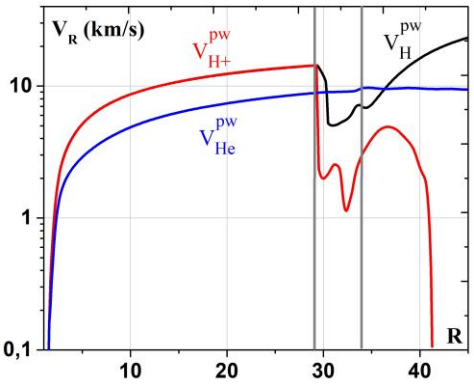

Fig.2 Profiles of density and velocity of the species in the PW across the planet-star line.

Acknowledgements

This work was supported by the Russian Science Foundation, project 18-12-00080, by the Russian Fund of Basic Research, project 16-52-14006, SB RAS basic research program (project II.10 №0307-2017-0015), and the Austrian Science Foundation FWF, projects I2939-N27, S11606-N16, S11607-N16. Parallel computing simulations have been performed at Computation Center of Novosibirsk State University, SB RAS Siberian Supercomputer Center, and Supercomputing Center of the Lomonosov Moscow State University.

References

[1] I. F. Shaikhislamov, M. L. Khodachenko, H. Lammer, et al .2016, ApJ, 832,173

[2] M. L. Khodachenko, I. F. Shaikhislamov, H. Lammer, et al. 2017, ApJ, 847,126

EPSC Abstracts
Vol. 12, EPSC2018-151, 2018
European Planetary Science Congress 2018

Global 3D multi-fluid aeronomy simulation of the HD 209458b

I. F. Shaikhislamov[1], M. L. Khodachenko[2,3], Tarek Al-Ubaidi[2], H. Lammer[2], A.G. Berezutsky[1], I.B. Miroshnichenko[1] and M.S. Rumenskikh[1]

(1) Institute of Laser Physics SB RAS, Novosibirsk, Russia, ildars@ngs.ru (2) Space Research Institute, Austrian Acad. Sci., Graz, Austria, (3) Skobeltsyn Institute of Nuclear Physics, Moscow State University, Moscow, Russia

Abstract

Using a global 3D, fully self-consistent, multi-fluid gas-dynamic aeronomic model, we simulate the dynamically expanding upper atmosphere of an exoplanet HD 209458b. The complex spatial structure of the escaping upper atmospheric planetary material, energized by the stellar XUV and driven further by tidal forces, while interacting with the stellar wind plasma is revealed in course of the modelling. We calculate transit absorption in Lyα and find that it is produced by both, dense exosphere inside the Roche lobe, due to the natural line broadening mechanism, and by the fast Energetic Neutral Atoms (so-called ENAs) outside the Roche lobe, due to the resonant thermal line broadening.

1. Introduction

Spectrally resolved transit measurements revealed extended planetary exospheres existing around a number of close-orbit exoplanets. Observed absorption in Lyα and resonant lines of heavier species, e.g., O, C in HD209458b indicates the dynamical expansion of its exosphere and overflowing the Roche lobe. Numerical simulation of this process involves aeronomy processes to describe the heating, chemical transformation and acceleration of the upper atmosphere in the form of an expanding planetary wind (PW) on one hand, and the interaction the PW with the stellar wind (SW) plasma on the other hand. So far the aeronomy simulations have been restricted to 1D models, while global 3D codes of the PW-SW interaction lacked the self-consistency regarding the modeling of the PW formation. Here we present a 3D multi-fluid gasdynamic model, which self-consistently simulates the global dynamics of the expanding PW within the SW environment.

2. The Model

We upgrade our previous 2D model (*Shaikhislamov et al. 2016, Khodachenko et al. 2017*) to a 3D case while keeping included all the details of the aeromomy of upper atmosphere, composed of hydrogen and helium. Using a sufficiently detailed planet based spherical coordinate system with a variable mesh, it is possible to resolve the wavelength- and height- dependent absorption of the ionizing stellar XUV radiation and the molecular hydrogen photo-chemistry in the highly stratified upper atmosphere of the HD209458b. Besides of that, the model simulates the expansion of the PW beyond the Roche lobe and its interaction with the SW under the action of inertia and gravity forces in a large spatial volume extending far beyond the planet orbit. This interaction also includes the generation of ENAs due to charge-exchange of slow planetary hydrogen with fast stellar protons, as well as stellar radiation pressure by the absorbed Lyα flux. For the reproducing of realistic SW parameters and calculation of the shock, formed during the SW-PW interaction, we use the adiabatic specific heats ratio 5/3, instead of the isotropic or polytropic ones, taken in the most of other global models. To sustain the continuous acceleration of the SW, an empirical heating of the stellar plasma inside the orbit ~0.1 a.u. is introduced. By taking certain values for the coronal temperature and density, as the boundary condition, either a slow, or a fast SW regimes can be modeled.

3. Results

We present here our first results on the simulation of the global structure of the dynamical plasma environment around HD 209458b under the conditions of the stellar XUV flux and SW typical for the Sun, and expected for a Sun-like star HD209458. Figure 1 shows the 3D plots of proton density and temperature. The planetary material stretches along

the orbit ahead and behind the planet. The SW overflows this structure and forms a shock along the whole length of the ahead streaming part of the PW flow. Due to the SW-PW interaction some planetary material is swept away by the SW.

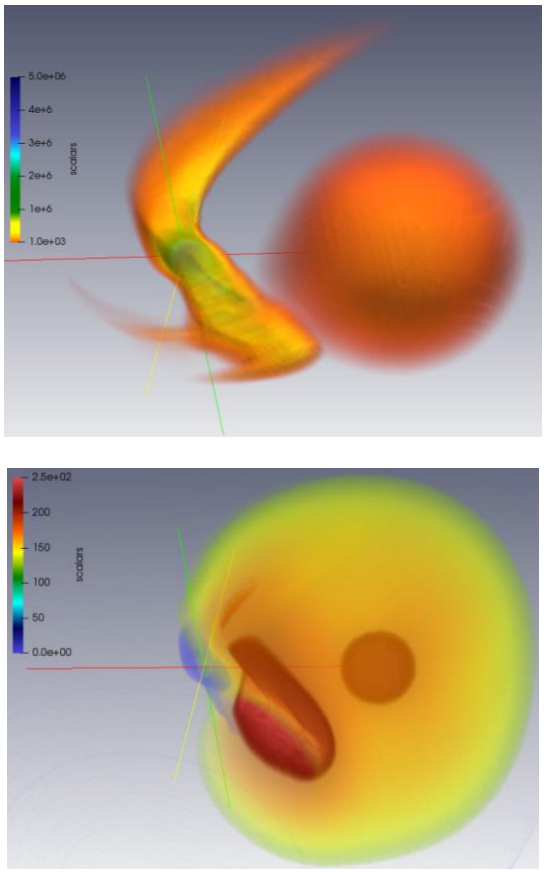

Figure 1: 3D color plots of proton density (upper panel, in cm^{-3}) and temperature (bottom, in units of 10^4 K). The coordinate axes are centered at the planet.

The profiles of the physical quantities along the planet-star line sown in Figure 2, demonstrate a sharp separation of the whole region onto planetary and star dominated domains. The H_2 dissociation front is located at about $1.5R_p$. The maximal temperature of the expanding PW reaches 9000 K at about $2R_p$, while velocity gets up to 40 km/s.

The calculated transit absorption in Lyα reveals that the main contribution comes from the natural line broadening mechanism, operating in the dense planetary exosphere inside the Roche lobe. The resonant Lyα absorption by ENAs (mostly at the blue wing of the line) might be also important, depending on the intensity of XUV flux and the density of SW plasma. This is in general agreement with our previous findings with the 2D axisymmetric model (*Khodachenko et al. 2017*). However, the essentially 3D geometry of the planetary plasma environment shows the new qualitative features and quantitative details, which can be captured only with the self-consistent 3D multi-fluid simulations.

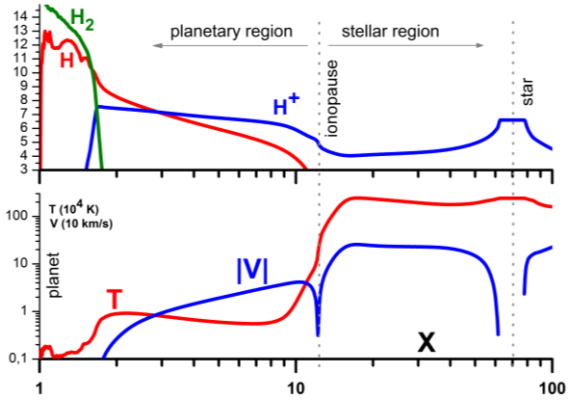

Figure 2: Density profiles for protons, molecular and atomic hydrogen (upper panel, log scale, in cm^{-3}); temperature and velocity distributions (bottom) along the planet-star line.

Acknowledgements

This work was supported by the Russian Fund of Basic Research project 16-52-14006, SB RAS basic research program (project II.10 №0307-2017-0015), and Austrian Science Foundation FWF, projects I2939-N27, S11606-N16, S11607-N16. Parallel computing have been performed at Computation Center of Novosibirsk State University, SB RAS Siberian Supercomputer Center, and Supercomputing Center of the Lomonosov Moscow State University.

References

[1] Shaikhislamov, I. F., Khodachenko, M. L., Lammer, H., et al. ApJ, 2016, 832(2), 173.

[2] Khodachenko, M. L., Shaikhislamov, I. F., Lammer, H., et al. ApJ, 2017, 847(2), 126.

EPSC Abstracts
Vol. 12, EPSC2018-158, 2018
European Planetary Science Congress 2018

Modeling of the UV absorption by OI and CII in exosphere of the hot jupiter HD 209458b

I.B. Miroshnichenko[1,2], I. F. Shaikhislamov[1], M. L. Khodachenko[3,4], H. Lammer[3], A.G. Berezutsky[1]

(1) Institute of Laser Physics SB RAS, Novosibirsk, Russia, ildars@ngs.ru (2) Novosibirsk State Technical University, Novosibirsk, Russia (3) Space Research Institute, Austrian Acad. Sci., Graz, Austria, (4) Skobeltsyn Institute of Nuclear Physics, Moscow State University, Moscow, Russia

Abstract

We apply a 2D hydrodynamic multi-fluid code [1, 2] to model the absorption in resonant lines of OI and CII in exosphere of HD 209458b. The absorption in these lines at the level of 10% was observed during several transits, but has not been yet satisfactorily explained. Our simulations show that the upper atmosphere of HD 209458b expands beyond the Roche lobe in the form of two supersonic streams that propagate towards and outwards the star. The heavier species of O and C are dragged within these streams and produce resonant Doppler shifted absorption consistent with the observations.

1. Introduction

Besides Lyα, the primary transit of HD209458b has been also observed with HST/STIS at other far UV wavelengths. In particular, *Vidal-Madjar et al.* (*2004*) reported absorption depths of 13±4.5% and 7.5±3.5% in OI ($2p^2$ 2P – $2p^2$ 2D) and CII ($2p^4$ 3P – $2p^4$ 3S) resonance lines. While the Lyα absorption may be dominated by the natural line broadening mechanism, acting in the exospheric material inside the Roche lobe, the absorption by heavier species, with the abundances 3 to 5 orders of magnitude less than that of hydrogen, offers a possibility to trace the planetary plasma beyond the Roche lobe. However, the previously applied 1D models could not explain the observed absorption width by the resonant broadening, corresponding to the width of the emission lines, up to 40 km/s, while the natural line broadening gave the absorption at the level of only 3-4%. *Koskinen et al.* (*2010*) estimated that such factors as sporadic hot spots on the stellar disk, limb darkening or limb brightening, super-solar abundances, position of H_2/H dissociation front can't provide sufficient increase of the OI transit depth, while *Ben-Jaffel & Sona Hosseini* (*2010*) argued that for the sufficient thermal broadening, O and C inside the Roche lobe should have temperatures up to 10 times higher than that of hydrogen. In the present paper we show that the observed broadening may be generated by a global flow of the escaping planetary upper atmospheric material beyond the Roche lobe.

2. The Model

The minor species were added to the initial atmosphere of the HD209458b, assuming the solar abundances, and then evolved according to the dynamic equations of the used model. The population of different ionization states for each element was calculated assuming the specific photo-ionization and recombination rates. Besides of that, an influence of the resonant charge-exchange reaction with hydrogen $O+H^+ \leftrightarrow O^+ + H$ on the atomic oxygen population was taken into account. The reaction cross-section, $\sim 10^{-15}$ cm^2, is sufficiently large, so that O ionization follows the ionization of H. Because of a much smaller photo-ionization threshold for C, than that for H, the carbon atoms are ionized in the lower thermosphere at heights of about $1.1R_p$. Therefore, we add the already ionized carbon atoms to the modelled atmosphere and follow the dynamics of CII and CIII, taking into account their further photo-ionization and recombination.

3. Results

Figure 1 shows density distributions of hydrogen atoms, OI and CII in the escaping planetary atmosphere of HD209458b. The assumed abundances for O and C are $O/H=8.5\cdot10^{-4}$ and $C/H=3.6\cdot10^{-4}$, respectively. The stellar wind (SW) was taken to be very weak, so that it does not affect the numerical solution for the outflowing planetary wind (PW). In our previous simulations [1, 2] it was shown that in case of neglecting the Coriolis force, the expanding PW forms a nearly symmetric double stream structure. Beyond the super-sonic transition point located outside the Roche lobe at $\sim 5R_p$, the

escaping PW streams are further accelerated by the tidal force.

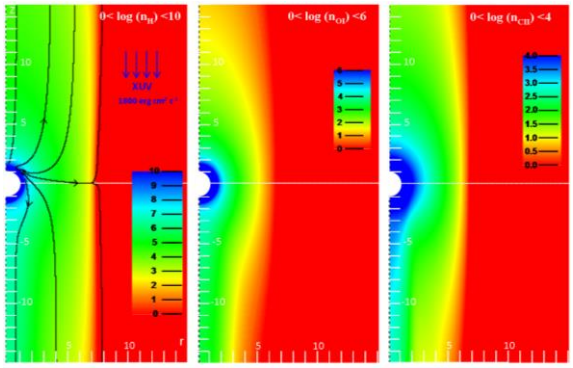

Figure 1. Density distributions of hydrogen atoms (n_H), oxygen atoms (n_{OI}) and carbon ions (n_{CII}) in the PW flow under typical for HD209458b conditions and for a very weak SW. The plotted values are in log scale. The streamlines of the corresponding flows are shown in black. The values outside the indicated variation ranges of the plotted parameters are colored either in red if smaller than minimum, or in blue, if higher than maximum. White circle indicates the planet.

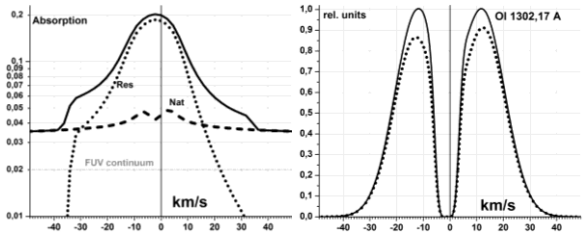

Figure 2. *Left panel*: The absorption profile for OI 1302.17 Å line (thick solid line). The dotted and dash-dotted lines show the decomposition of the OI 1302.17 Å line absorption onto the resonant component and the absorption due to natural line broadening, respectively. *Right Panel*: The shape of OI 1302.17 Å line out-of-transit (solid) and the modeled in-transit (dotted), depleted due to absorption.

The absorption produced by OI, carried within the PW flow, is shown in Figure 2 for the case of the line OI 1302.17 Å, taken as an example. It produces the largest contribution to the whole absorption of the OI multiplet, because of its highest statweight. The decomposition of the calculated absorption shows that its resonant part constitutes a significant portion (5÷15) %, covering almost the whole line from –30 km/s in the blue wing up to 15 km/s in the red wing. The input of natural line broadening by dense exosphere is about 4%, which is the same as in previous works where no PW motion was included. The transit depth of the whole OI multiplet reaches a value of 8.5%. The similarly modeled CII multiplet absorption gets up to 8.7%. In the simulations we also checked how the absorption is affected by such factors as XUV intensity and SW intensity. It was found that sufficiently high total pressure of the SW may stop the dayside PW flow, making the absorption profile strongly asymmetric. This effect enables the probing of the SW intensity.

It has been shown for the first time that with the account of the effect of the species, carried within escaping PW streams, the transit depths observed for oxygen and carbon resonant multiplets can be reproduced assuming the typical solar abundances. The depths can be even larger than that for the Lyα line, reaching values of about 10%. The performed simulations confirm the previously proposed idea that bulk motion of the HD209458b hydrogen atmosphere, escaping the planet with the velocity of several tens of km/s, drags the heavy elements, which sufficiently increase the resonant line broadening in absorption of the corresponding stellar lines.

Acknowledgements

This work was supported by the Russian Science Foundation, project 18-12-00080 and Austrian Science Foundation FWF, projects I2939-N27, S11606-N16, S11607-N16. Parallel computing simulations have been performed at Computation Center of Novosibirsk State University, SB RAS Siberian Supercomputer Center, and Supercomputing Center of the Lomonosov Moscow State University.

References

[1] Shaikhislamov, I. F., Khodachenko, M. L., Lammer, H., Kislyakova, K. G., Fossati, L., Johnstone, C. P., ... & Posukh, V. G. Two regimes of interaction of a Hot Jupiter's escaping atmosphere with the stellar wind and generation of energized atomic hydrogen corona. The Astrophysical Journal, 832(2), 173, 2016.

[2] Khodachenko, M. L., Shaikhislamov, I. F., Lammer, H., Kislyakova, K. G., Fossati, L., Johnstone, C. P., ... & Posukh, V. G. Lyα Absorption at Transits of HD 209458b: A Comparative Study of Various Mechanisms Under Different Conditions. The Astrophysical Journal, 847(2), 126, 2017.

EPSC Abstracts
Vol. 12, EPSC2018-237, 2018
European Planetary Science Congress 2018

Influence of the dipolar magnetic field on the hot jupiter envelopes

Dmitry Bisikalo
Institute of astronomy of the Russian Academy of Sciences (bisikalo@inasan.ru)

Abstract

In this report we discuss possible influence of the proper magnetic field on the gaseous envelopes of hot jupiters.

1. Introduction

Hot jupiter exoplanets, have a number of outstanding features, caused mostly by their proximity to the host star, e.g.: gas outflowing from the planet's atmosphere to the star, as it happens in close binary stars. Gas-dynamical modeling shows that, if the dynamical pressure of the stellar-wind is high enough to stop the outflow from the vicinity of the inner Lagrangian point, a quasi-closed non-spherical envelope, bounded by the bow-shock of a complex shape, forms in the system. The aim of our current study is to estimate the possible variations of the structure and dynamics of flows in the envelope of a hot jupiter due to the presence of the planetary magnetic field.

2. Reduction of mass loss due to hot jupiter magnetic field

The results of three-dimensional MHD computations of a hot jupiter with the parameters of the object WASP-12b [1] show that the presence of a magnetic field leads to appreciable variations of the matter flow structure. In the solution without magnetic field, the overflow of the Roche lobe by the planetary atmosphere leads to the formation of an open envelope with a mass-loss rate of ~1.5 10^{10} g/s. In spite of the fairly weak magnetic field of the planet (a strength of ~0.1 the magnetic moment of Jupiter), the MHD solution differs appreciably from the purely gas-dynamical solution: for the same parameters of the atmosphere, the propagation of the stream from the vicinity of L_1 occurs perpendicular to the magnetic-field lines and is stopped by the pressure of the stellar wind at a distance of ~14 R_{pl} from the planet, forming a quasi-closed envelope. The mass-loss rate in the solution with the magnetic field was ~4 10^9 g/s. This reduction (by ~70%) of the mass-loss rate due to the influence of the magnetic field makes it possible for exoplanets to form closed and quasi-closed envelopes in the presence of more strongly overflowing Roche lobes than is possible without a magnetic field.

3. Pulsations in the envelopes of hot jupiters possessing magnetic fields

Three-dimensional MHD modeling on time scales appreciably exceeding the time for the formation of the envelope [2] show that the presence of a magnetic field appreciably changes the flow patterns in systems whose parameters lie within the range enabling the existence of quasi-closed envelopes. An important difference of the MHD flows from purely gas-dynamical flows is the existence of a pulsation regime for the outflow of matter. Pulsation in the outflow of matter through the inner Lagrange point L_1 arises when the outflowing gas cannot simultaneously overcome the dynamical pressure of the wind and the tension of the magnetic-field lines. In this case, the gas accumulates in regions surrounded by closed magnetic-field lines until there is a rupture in the direction toward the star (in the vicinity of L_1), during which the accumulated matter forms a flow. The stream that is formed shields the vicinity of L1 from the stellar wind, making it possible for the flow to recover. After the re-establishment of the flow, the matter in the vicinity of L_1 rapidly dissipates, and the tension of the magnetic-field lines again becomes sufficient to confine the matter, leading to a new cessation of the flow. After the dissipation of the stream, the stellar wind finally closes off the vicinity of L_1, and the cycle of the accumulation of matter begins again.

Computations conducted for a dipolar field geometry with the dipole axis oriented perpendicular to the orbital plane have shown that the pulsation period for the solution with magnetic moment $\mu = 0.125\mu_{Jup}$ is ~0.27 of the orbital period. This pulsational outflow

regime should substantially influence the observational manifestations of the extended envelopes of hot jupiters.

4. Summary and Conclusions

The discovery of the possible existence of huge quasi-stationary envelopes around a number of hot jupiters (i.e., with sizes appreciably exceeding their Roche lobes) and the need to correctly take into account their properties when interpreting observational data require a careful analysis of the main physical processes influencing their atmospheres. One important factor is the possibility that the planet has a magnetic field. It was shown that the presence of even a modest dipolar magnetic field of a hot jupiter (with a magnetic moment approximately 1/10 the magnetic moment of Jupiter) influences the properties of the planetary atmosphere, in particular, leading to expansion of the range of parameters for which a giant, quasi-closed envelope can form around the planet. It was also established that the presence of a planetary magnetic field reduced the mass-loss rate from the envelope, since matter flowing out from the inner Lagrange point moves perpendicular to the field lines.

Three-dimensional MHD modeling also show that pulsations arise in the atmospheres of hot jupiters possessing dipolar magnetic fields, with characteristic periods $\sim 0.27 P_{orb}$. In the case considered, when the system contains a giant envelope fed by a stream of matter from the inner Lagrange point, the presence of such pulsations gives rise to appreciable variations in the gas-dynamical structure of the flow. In particular, pulsations of the atmosphere lead to tearing off of part of the flow and sharp fluctuations in the size of the envelope, leading to variations in the envelope's observational properties.

Acknowledgements

This work was supported by the Russian Science Foundation (Project 18-12-00447).

References

[1] Arakcheev, A.S., Zhilkin, A.G., Kaigorodov, P.V., Bisikalo, D.V. and Kosovichev, A.G.: Reduction of mass loss by the hot Jupiter WASP-12b due to its magnetic field, Astronomy Reports, Vol.61, pp. 932-941, 2017.

[2] Bisikalo, D.V., Arakcheev, A.S. and Kaigorodov, P.V.: Pulsations in the atmospheres of hot Jupiters possessing magnetic fields, Astronomy Reports, Vol.61, pp. 925-931, 2017.

EPSC Abstracts
Vol. 12, EPSC2018-240, 2018
European Planetary Science Congress 2018

Modelling observability of Star-planet interaction

C. Fischer, J. Saur
Institute of Geophysics and Meteorology, University of Cologne (fischer@geo.uni-koeln.de)

Abstract

Exoplanets sufficiently close to their host star can couple electromagnetically to the star. This process is known as electromagnetic star-planet interaction (SPI). So far there is no clear observational evidence for SPI because of the usually bright intrinsic stellar emissions. We apply semi-analytic approaches to model the properties of SPI. The understanding of basic physical phenomena could help to identify signals of SPI in stellar lightcurves. We chose the TRAPPIST-1 system for our studies. Its seven planets make it an intriguing system for the search of SPI. We show that SPI is possible in this system and discuss its observability.

EPSC Abstracts
Vol. 12, EPSC2018-281, 2018
European Planetary Science Congress 2018

In-transit Lyα absorption by HD 209458b under different regimes of the planetary and stellar winds interaction

M. L. Khodachenko [1,2], I. F. Shaikhislamov[3], N. Dwivedi[1], H. Lammer[1], K. G. Kislyakova[4], L. Fossati[1], C. P. Johnstone[4], O.V. Arkhypov[1], A. G. Berezutsky[3], I.B. Miroshnichenko[3], Posukh[3] V. G.

(1) Space Research Institute, Austrian Acad. Sci., Graz, Austria (maxim.khodachenko@oeaw.ac.at) (2) Skobeltsyn Institute of Nuclear Physics, Moscow State University, Moscow, Russia (3) Institute of Laser Physics SB RAS, Novosibirsk, Russia (4) Dep. of Astrophysics, University of Vienna, Austria

Abstract

The interaction of an escaping upper atmosphere of a hydrogen rich non-magnetized analogue of HD209458b with the stellar wind of its host G-type star is simulated with a 2D axisymmetric multi-fluid hydrodynamic model. Different regimes of the planetary upper atmospheric material escape, depending on the parameters of the stellar wind and XUV flux are considered. The performed simulations enable calculating of the Lyα absorption during transits of HD209458b and quantifying the major mechanisms responsible for its observed features.

1. Introduction

The interpretations of Lyα spectra measured during transits of HD209458b still remain controversial. The existing explanations based on 1D hydrodynamic models of hot Jupiters' material escape suggest that the detected absorption, extending over the high velocity wings (~100 km/s), is due to *non-resonant natural line broadening*, caused by dense and warm exosphere that fills the Roche lobe of the planet. At the same time, the modelling by kinetic codes yields that the *resonant, or thermal line broadening* absorption by fast hydrogen atoms, so-called ENAs, which takes place beyond the Roche lobe might be more important. As the major mechanisms responsible for the ENAs production, the acceleration by radiation pressure (in the same Lyα band) and charge-exchange between stellar wind protons and planetary atoms are considered, while the domination of particular mechanism is still the matter of debate. To shed more light on that issue, we apply a 2D hydrodynamic multi-fluid model that self-consistently describes the expansion of a "hot jupiter's" upper atmosphere composed of hydrogen and helium at partial ratio $x_{He}/x_{H2} = 1/5$ (heated by the stellar XUV), taking into account the interaction between the expanding planetary wind and the stellar wind plasma. The production of ENAs by charge-exchange and acceleration by the radiation pressure are taken into account in the model [1,2].

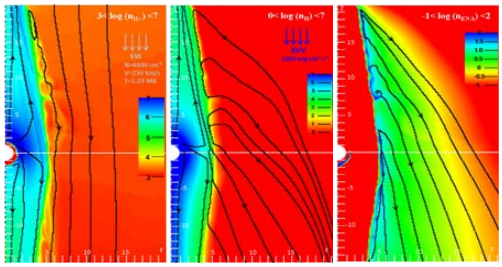

Figure 1: Density distributions of protons (n_{H+}), planetary atoms (n_H) and ENAs (n_{ENA}), in the *"captured by the star"* regime of PW-SW interaction by HD209458b for the *slow* SW (p_{SW}=5x10^{-6} μbar), F_{XUV}=4.466 erg s^{-1}cm^{-2} at 1 a.u.

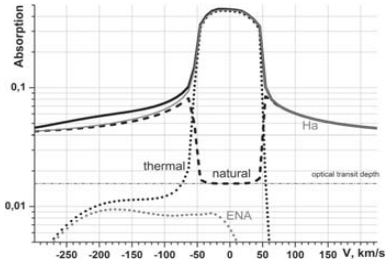

Figure 2: Absorption profile of Lyα line (thick solid) for the regime sown in Figure 1. Black-dotted and black-dashed lines represent the *resonant thermal* and *non-resonant natural* parts of the absorption, respectively; whereas gray-dotted and gray-solid lines show the contribution of ENAs and planetary atomic hydrogen (Ha).

2. Results

Depending on natural (about an order of magnitude) variations in the total pressure of the stellar wind SW,

the escaping planetary wind (PW) of HD209458b formed during the expansion of the planetary upper atmosphere energized by the stellar XUV radiation, can exist in two essentially different regimes [1]: 1) the "*blown by the wind*" regime, when sufficiently strong SW stops the escaping PW at the day-side and channels it away from the star into the tail, forming a kind of a paraboloid-shaped planetary plasmasphere, and 2) the "*captured by the star*" regime, when the tidal force exceeds the action of the SW ram pressure and a double-stream structure of the escaping PW is formed along the planet-star line (in the star-wards and tail-wards directions). In both cases the PW is sufficiently dense to remain strongly collisional even rather far from the planet (up to several tens of R_p).

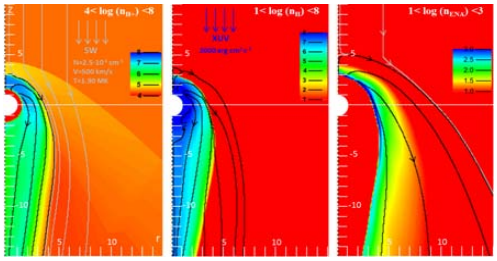

Figure 3: Density distributions of protons (n_{H+}), planetary atoms (n_H) and ENAs (n_{ENA}), in the *"blown by the wind"* regime of PW-SW interaction by HD209458b for the *fast* SW (p_{SW}=1.3x10^{-4} μbar), F_{XUV}=4 erg s^{-1}cm^{-2} at 1 a.u.

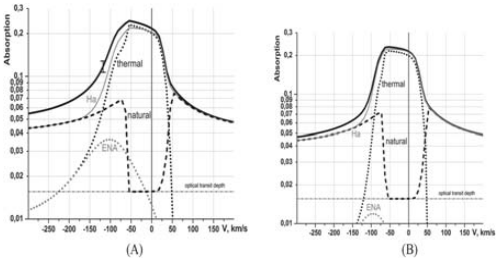

Figure 4: Absorption profile of Lyα line (thick solid) in the *"blown by the wind"* regime of PW-SW interaction by HD209458b for the *fast* SW (500km/s, T_{SW}=2.9MK). **(A)**: F_{XUV}=4 erg s^{-1}cm^{-2} at 1 a.u., n=2.5x10^{4}cm^{-3}; **(B)**: F_{XUV}=8 erg s^{-1}cm^{-2} at 1 a.u., n=5x10^{4}cm^{-3}.

The distributions of density of protons, planetary hydrogen atoms and ENAs realized in the "*captured by the star*" regime of PW-SW interaction for the *slow* SW under the typical for HD209458b conditions, and the decomposition of the corresponding Lyα absorption profile onto the *resonant thermal* and *non-resonant natural* with showing also the contribution of ENAs and planetary atomic hydrogen, is presented in Figures 1 and 2, respectively. The results of similar study for the case of the *"blown by the wind"* regime of PW-SW interaction are shown in Figures 3 and 4.

3. Conclusions

It has been demonstrated that the most crucial factor affecting the ENA environment of HD209458b is the XUV flux. At the same time, the calculations in a wide range of stellar wind parameters and XUV flux values have shown that under the typical conditions expected for HD209458b the amount of generated ENAs is too small, and the observed absorption at the level of 6÷8% can be attributed only to the *non-resonant natural line broadening*. For lower XUV fluxes, e.g., during the activity minima, the number of planetary atoms that survive photo-ionization and give the origin to ENAs, increases resulting in up to 10÷15% absorption at blue wing of Lyα line, caused by *the resonant thermal line broadening*. Similar asymmetric absorption can be seen under the conditions of a fast SW with a sufficiently high total pressure, e.g. during Coronal Mass Ejections, when the escaping PW flow is confined the within a kind of bowshock around the planet. It has been found, that the radiation pressure in all considered cases has a negligible contribution to the production of ENAs and the corresponding absorption.

Acknowledgements

This work was supported by the Austrian Science Foundation (FWF) projects I2939-N27, S11606-N16, S11607-N16, the Russian Fund of Basic Research (project 16-52-14006), and SB RAS basic research program (project II.10 №0307-2017-0015). Parallel computing simulations have been performed at Computation Center of Novosibirsk State University, SB RAS Siberian Supercomputer Center, and Supercomputing Center of the Lomonosov Moscow State University.

References

[1] Shaikhislamov, I. F., Khodachenko, M. L., Lammer, H., et al. ApJ, 2016, 832(2), 173.

[2] Khodachenko, M. L., Shaikhislamov, I. F., Lammer, H., et al. ApJ, 2017, 847(2), 126.

EPSC Abstracts
Vol. 12, EPSC2018-303, 2018
European Planetary Science Congress 2018

Multi-fluid modeling of upper atmosphere mass loss and absorption line for WASP-12b

Navin Dwivedi (1), Ildar Shaikhislamov (2), Maxim Khodachenko (1,3), Luca Fossati (1), Helmut Lammer (1), Kristina Kislyakova (4), Collin Johnstone, Manuel Güdel (4) and Yuri Sasunov (1)
(1) Space Research Institute, Austrian Academy of Sciences, Graz, Austria, (2) Institute of Laser Physics SB RAS, Novosibirsk, Russia, (3) Skobeltsyn Institute of Nuclear Physics, Moscow State University, Moscow, Russia, (4) Department of Astronomy, University of Vienna, Austria (Navin.Dwivedi@oeaw.ac.at)

Abstract

The work presents the multi-fluid numerical modeling to interpret the observed absorption in Mg_{II} resonance lines during the transit of WASP-12b and to quantify the crucial mechanisms responsible for exoplanetary upper atmosphere mass loss. The model simulates the expansion of upper atmosphere due to stellar XUV radiation and includes the hydrogen chemistry and effects of stellar wind. The two case-scenarios of the planetary material escape and interaction with the stellar wind, namely the 'blown by the wind' (without the inclusion of tidal force) and 'captured by the star' (with the tidal force) have been modeled for different stellar XUV radiation fluxes and different stellar wind parameters. In the first case, the planetary mass loss is controlled completely by the stellar radiation energy input. However, in the 'captured by the star' case, the mass loss is mainly due to the gravitational interaction effects. The dynamics of Mg_{II} ions was modeled with three different sets of stellar wind parameters and XUV flux values under a realistic Sun-like star condition. The results appear in good agreement with the observations.

1. Introduction

WASP-12b is one of the recently observed close-orbit, short period hot Jupiters [1, 2]. The Roche lobe size of the planet is a little larger than the planet radius, and therefore the planet mass loss due to tidal force has to be a very common phenomenon for this planet. Fossati et al. [2] and Haswell et al. [3] investigated two transits of the planet and advocated the likelihood of early ingress in the near-UV of the planet compared to its optical light curve which is reminiscent of absorbing material around the planet. Fossati et al. [2] and Nochols et al. [4] have detected an extra absorption in the Mg_{II} resonance line cores at the 2.8σ level.

The main objective of the present work is to analyze the two scenario namely the formation of bow-shock and diffused cloud or torus due to the material escape from the planetary exosphere to understand the observed phenomenon of early ingress, extra absorption in Mg_{II} resonance line and mass loss processes.

2. Multi-fluid Simulation results

A 2D multi-fluid model developed in [5, 6] is adopted for the specific case of WASP-12b. In the 'blown by the wind' case, the stellar wind (SW) total pressure is sufficiently high enough to stop the planetary wind (PW), and to create an ionopause, and a bow shock. However, in the 'captured by the star' case, the PW expands beyond the Roche lobe towards the star being further pulled by the tidal force. Figures 1 and 2, illustrate the density distribution of the main interacting constituents, respectively for the case of 'blown by the wind' and 'captured by the star' regimes. The simulated absorption profiles of Mg_{II} line for the magnesium abundance Mg/H=3.7x10^{-5}are shown in Fig. 3, for the both regimes.

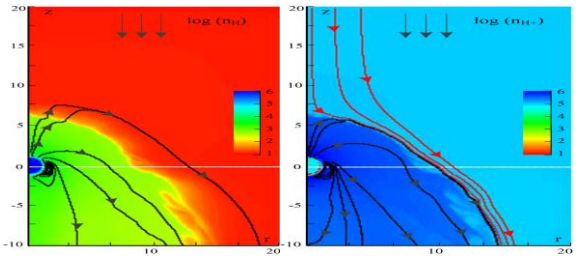

Figure 1. The density distribution of planetary atoms, ions and stellar protons in the case of 'blown by the wind'regime for F_{XUV}=5ergcm^{-2}s^{-1}, n_{SW}=310^{4}cm^{-3}, T_{SW}=1.4MK, and V_{sw}=172kms^{-1}.

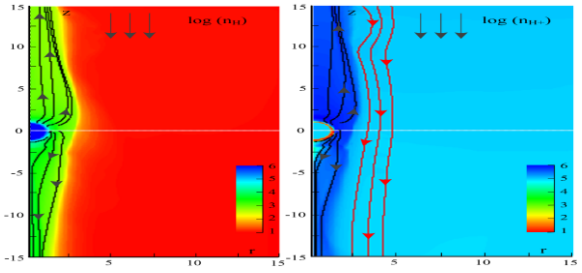

Figure 2. The density distribution of planetary atoms, ions and stellar protons for the case of 'captured by the star by the wind' regime for F_{XUV}=5ergcm^{-2}s^{-1}, n_{SW}=1x10^{4}cm^{-3}, T_{SW}=3.17MK, and V_{sw}=417kms^{-1}.

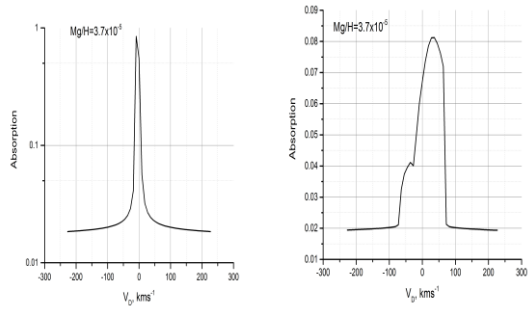

Figure 3. Absorption profile of Mg_{II} line calculated at magnesium abundance of Mg/H=3.7x10^{-5}, for the cases of 'blown by the wind' and 'captured by the star' regimes respectively.

3. Mass loss

The average mass loss rate values for different SW-PW interaction regimes are summarized in Table 1 and Table 2 respectively.

Table 1: 'Blown by the wind' regime

F_{XUV} (ergcm^{-2}s^{-1})	n_{SW} (cm^{-3})	V_{SW} (kms^{-1})	T_{SW} (MK)	Mass loss rate (10^{10}gs^{-1})
5	3x10^{4}	172	1.4	28.81
10	6x10^{4}	172	1.4	49.10
20	6x10^{4}	172	1.4	88.87

Table 2: 'Captured by the wind' regime

F_{XUV} (ergcm^{-2}s^{-1})	n_{SW} (cm^{-3})	V_{SW} (kms^{-1})	T_{SW} (MK)	Mass loss rate (10^{10}gs^{-1})
5	1x10^{4}, 3x10^{4}	417	3.17	145.38, 222.98
10	1.5x10^{4}, 3x10^{5}	417	3.17	169.95, 197.64
20	1.5x10^{4}, 3x10^{5}	417	3.17	186.53, 225.29

4. Summary and Conclusions

The simulation results demonstrate that in the 'blown by the wind' regime when a slow SW condition and no tidal force is considered in the model, we observe a very strong absorption of Mg_{II}. However, in the 'captured by the star' regime, we found that the change in the XUV radiation fluxes does not make a significant change in the absorption profile of Mg_{II} line. However, the SW condition has a major impact on the Mg_{II} absorption line. In the case of 'captured by the star' regime, the calculated absorption shows a good agreement with the observed value of absorption in Mg_{II} line which is 3-4%.

Acknowledgments

This work was supported by the Austrian Science Foundation (FWF) project I2939-N27, FWF-NFN projects S11606-N16, S11607-N16 and the Russian Science Foundation grant № 18-12-00080 and SB RAS basic research program (project II.10 № 0307-2017-0015).

References

[1] Hebb, L., Collier-Cameron, A., and Loeillet, B. et al., APJ, 693, 1920-1928, 2009.
[2] Fossati, L., Haswell, C. A., and Froning, C. S. et al., APJ Letts., 714, L222-L227, 2010.
[3] Haswell, C. A., Fossati, L., and Ayres, T. et al., APJ, 760, 79, 2012.
[4] Nichols, J. D., Wynn, G. A., and Goad, M. et al., APJ, 803, 9, 2015.
[5] Shaikhislamov, I. F., Khodachenko, M. L., and Sasunov, Yu L. et al., APJ, 795, 132, 2014.
[6] Khodachenko, M. L., Shaikhislamov, I., and Lammer, H. et al., APJ, 847, 126, 2017.

EPSC Abstracts
Vol. 12, EPSC2018-461-1, 2018
European Planetary Science Congress 2018

Observations of fast-moving structures in the debris disk of AU Microscopii: A possible case of star-planet interactions at large orbital distances

Anthony Boccaletti (1), Elie Sezestre (2), Anne-Marie Lagrange (2), Philippe The´bault (1), and the SPHERE consortium
(1) LESIA, Observatoire de Paris, PSL Research Univ., CNRS, Univ. Paris Diderot, Sorbonne Paris Cité, UPMC Paris 6, Sorbonne Univ., 5 place Jules Janssen, 92195 Meudon, France(anthony.boccaletti@obspm.fr), (2) Univ. Grenoble Alpes, CNRS, IPAG, F-38000 Grenoble, France

Abstract

The extreme AO coronagraphic instrument SPHERE was installed at the VLT in 2014 and provides a significant gain in terms of contrast with respect to the previous generation of instruments. As a result, we now have access to very high contrast in the close environment of bright stars in particular the young systems in order to search for giant planets and circumstellar disks. During the commissioning in Aug 2014, SPHERE has revealed several structures (several AU in size) in the form of arches or undulations in the midplane of the debris disk around the M-type star AU Microscopii (Fig. 1). This disk is seen edge on and the system is conveniently close (10 pc) and young as well (20 Myr). The comparison of these SPHERE observations with the ones from STIS/HST 4 years before, not only allowed us to re-identify the structures in older data but most importantly led us to conclude that these structures were moving outwards in the disk, some with very large projected speed (4-10 km/s) hence possibly escaping the system. Several assumptions were considered to explain this behaviour, one of the them involves a body in Keplerian motion releasing some dust under the influence of the star's activity (Fig. 2). Since then, the target is regularly observed with SPHERE as part of the GTO and during a monitoring program. I'll remind the initial results from 2014 which led to the discovery of these fast-moving structures. Then, I'll present the recent observations obtained from the last 3 years which unambiguously confirm the motion of the structures. The hypothesis of a parent body orbiting the star and emitting an outflow of dust under the influence of the stellar wind will be discussed in the light of these observations. While star-planet interaction is widely admitted for close in planets, the modeling of our data suggests that interactions are also possible at much larger separations in the range 10-30 AU. The exact nature of the dust emission is still unexplained so the objective of this presentation in this particular session is to foster exchange of ideas on this peculiar system.

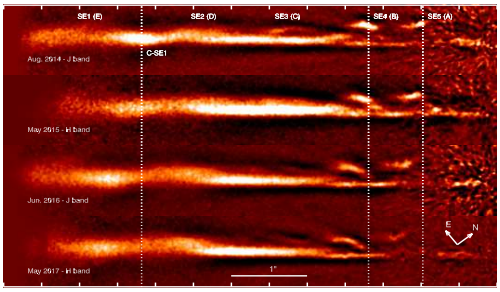

Figure 1: SPHERE/IRDIS total intensity images of the southeast side of the disk for the four best epochs (Aug. 2014, May 2015, Jun. 2016, and May 2017). The data are multiplied with the stellocentric distance (to give more weight to the outer parts). The star is at the right of the image. The field of view is 6.5" $\times$ 1.0" , and the intensity scale is adapted for each epoch. Vertical dotted lines are drawn to roughly locate on the first epoch (Aug. 2014) the positions of the main features (SE5 and SE4 as well as an intensity enhancement C-SE1 at $\sim$4.7"). The top and bottom axes are graduated every 0.5″.

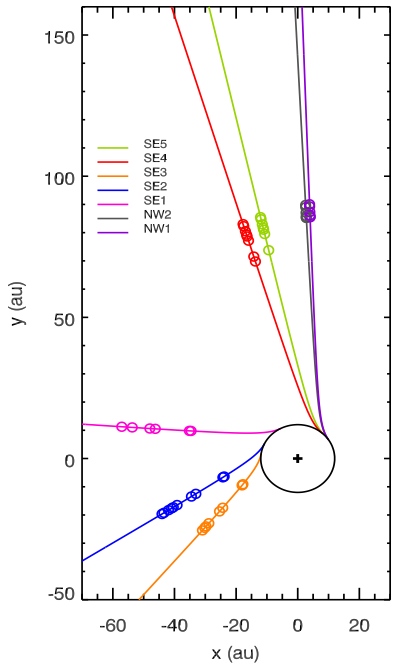

Figure 2: Face-on view of possible trajectories of the structures if they were emitted from a object orbiting the star (black circle). For each structure, a circle materializes the stellocentric position calculated from the model at the epochs when the structure is detected. The observer is at the bottom. Counter-clockwise rotation is assumed.

EPSC Abstracts
Vol. 12, EPSC2018-641-1, 2018
European Planetary Science Congress 2018

Influence of Star-Planet Magnetic Torques on Orbital Secular Evolution

Jérémy Ahuir (1), Antoine Strugarek (1), Mansour Benbakoura (1), Allan-Sacha Brun (1), Stéphane Mathis (1), Emeline Bolmont (1), Christophe Le Poncin-Lafitte (2), Victor Réville (3)

(1) Laboratoire AIM Paris-Saclay, CEA/Irfu Université Paris Diderot CNRS/INSU, Gif-sur-Yvette, France, (2) LNE-SYRTE, Observatoire de Paris, PSL Research University, CNRS, Sorbonne Universités, UPMC Univ. Paris 06, Paris, France, (3) UCLA Department of Earth, Planetary and Space Sciences, Los Angeles, CA, United States

Abstract

The discovery of more than 3000 exoplanets during the last two decades has shed light on the importance of characterizing star-planet interaction. We address this question by studying systems formed by a solar-like star and a close-in planet. We consider the joint influence on the star's rotation rate and planetary orbital evolution of a stellar wind, tidal and magnetic star-planet interactions. Despite recent significant advances in these fields, all current models use parametric descriptions to study at least one of these effects. Our objective is to introduce simultaneously ab-initio prescriptions of the tidal, braking and magnetic torques, so as to improve our understanding of star-planet systems and their long-term evolution.

To this end we develop a 1D numerical model of coplanar circular star-planet systems taking into account stellar structural changes, wind braking, tidal and magnetic interactions and implement it in a code called ESPEM (French acronym for Evolution of Planetary Systems and Magnetism). We follow the secular evolution of the stellar rotation assuming a bi-layer internal structure, and of the semi-major axis of the orbit. After comparing our predictions to recent observations and models, we perform tests to emphasize the contribution of ab-initio prescriptions. Finally, we isolate four significant characteristics of star-planet systems: stellar mass, initial stellar rotation period, planetary mass and initial semi-major axis; and browse the parameter space to investigate the influence of each of them on the fate of the system.

We find that depending on the characteristics of the system, tidal or magnetic effects can dominate. For very close-in planets, we find that both torques can make a planet migrate on a timescale as small as 10-100 thousands of years. Both effects thus have to be taken into account when predicting the evolution of compact systems. Finally, we provide a planet survival criterion based on the star-planet global parameters, determining whether or not the planet will undergo orbital decay due to tidal interaction and star-planet magnetic interaction.

EPSC Abstracts
Vol. 12, EPSC2018-802, 2018
European Planetary Science Congress 2018

On the transit Lyα observations of terrestrial planets in the habitable zones of M dwarfs

Kristina Kislyakova (1,2), Helmut Lammer (2), Petra Odert (2), Nikolai Erkaev (3,4), and Mats Holmström (5)
(1) University of Vienna, Department of Astrophysics (2) Space Research Institute, Austrian Academy of Sciences (3) Institute of Computational Modelling, Siberian Division of Russian Academy of Sciences, Krasnoyarsk, Russia (4) Siberian Federal University, Krasnoyarsk, Russia (5) Swedish Institute of Space Physics, Kiruna, Sweden (kristina.kislyakova@univie.ac.at)

Abstract

We study the transit signatures in the Lyman-alpha (Lyα) line of a putative Earth-sized planet orbiting in the habitable zone (HZ) of GJ 436. We estimate the transit depth in the Lyα line for an exo-Earth with three types of atmospheres: a hydrogen-dominated atmosphere, a nitrogen-dominated atmosphere, and a nitrogen-dominated atmosphere with an amount of hydrogen equal to the one of the Earth. We use out-of-transit observations of GJ 436 to study the calculated absorption.

1. Introduction

Lyα transit observations are a very important tool to study exoplanetary atmospheres. GJ 436 hosts a transiting Neptune-sized planet GJ 436b which has been observed in the Lyα line and revealed a very deep transit in this line, indicating a presence of a dense hydrogen envelope surrounding the planet [1]. Our aim is to check if a terrestrial planet in the HZ of an M star like GJ 436 can create observable signatures in the Lyα line in transit. To do so, we perform atmospheric modeling using Direct Simulation Monte Carlo (DSMC) code and then calculate Lyα absorption.

2. The model

We use a 3D DSMC code to model the extended atomic coronae of exoplanets. The code allows to track different species (up to 7 to date) as well as the interactions between species, and is able to handle different weights of the atomic metaparticles. The code is suitable for modeling of the rarefied planetary exospheres. The species are allowed to charge exchange with stellar wind protons as well as being photo- and electron impact ionized and collide with each other. The main processes and forces included for an exospheric atom are:

1. For hydrogen atoms: collision with a UV Lyα photon which defines the velocity-dependent radiation pressure. In this study, we consider relatively thin hydrogen envelopes. For this reason, self-shielding, i.e., optical depth in Lyα is not included. For non-hydrogen atoms, radiation pressure is not included.
2. Charge exchange with a stellar wind proton.
3. Elastic collision with another neutral atom.
4. Ionization by stellar photons or wind electrons. While being very important for hot Jupiters, in the HZ electron impact ionization is not significant due to a much less denser wind.
5. Gravity of the star and planet, centrifugal, Coriolis and tidal forces.

The code has been previously successfully applied to modeling of hydrogen-dominated atmospheres (e.g., [2]).

3. Modeling results

Fig. 1 presents our modeling of atomic coronae around a putative Earth-sized, Earth-mass planet orbiting in the HZ of GJ 436. The simulations are performed for three types of atmospheres: a hydrogen dominated atmosphere (left), a nitrogen dominated atmosphere with an additional hydrogen exospheric density equal to hydrogen density in the Earth's exosphere (center), and a fully nitrogen dominated atmosphere with no additional hydrogen content (right).

4. Summary and Conclusions

According to our results, only hydrogen-dominated atmospheres can be detected in the Lyα line for the quality of observations similar to out-of-transit observations of GJ 436. This indicates that secondary (non-

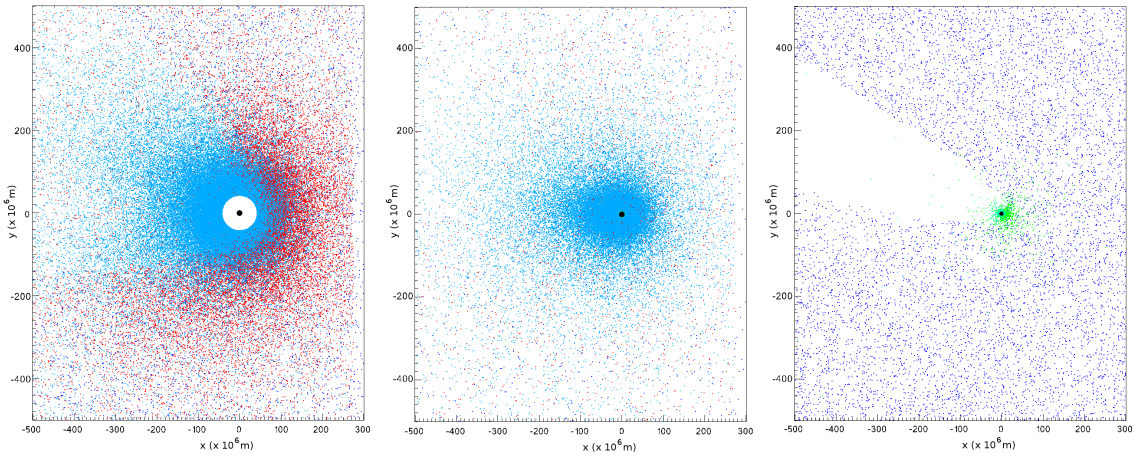

Figure 1: Illustration of modeled 3D atomic hydrogen coronae. Presented is a slice of modeled 3D domain for -10^6<z<10^6 m. Left: hydrogen-dominated atmosphere. Middle: nitrogen-dominated atmosphere with Earth-like hydrogen content. Right: fully nitrogen-dominated atmosphere. All dots show simulated metaparticles of the exosphere of a planet. The dark blue dots symbolize stellar wind protons, the light blue dots are the neutral atmospheric hydrogen particles, the green dots are neutral nitrogen atoms and ionized planetary N+. The red dots are ionized planetary hydrogen atoms (H+ of planetary origin). The black dot in the center of each plot is the planet, the white area around it is the lower atmosphere which is not simulated. For nitrogen-dominated atmospheres, the lower atmosphere is very close to the planetary surface, so that the white area is not visible on the plots due to scalings. The star is on the right, and the stellar wind is coming from the right side.

hydrogen dominated) atmospheres can be more effectively studied by other means. The results are being prepared for publication [3].

Acknowledgements

We acknowledge the support by the Austria Science Fund (FWF) NFN project S116-N16 and the subproject S11607-N16.

References

[1] Ehrenreich, P., Bourrier, V., Wheatley, P., et al.: A giant comet-like cloud of hydrogen escaping the warm Neptune-mass exoplanet GJ 436b, Nature, Vol. 522, p. 459, 2015.

[2] Kislyakova, K.G., Holmström, M., Lammer, H., et al.: Magnetic moment and plasma environment of HD 209458b as determined from Lyα observations, Science, Vol. 346, p. 981, 2014.

[3] Kislyakova, K.G., Holmström, M., Lammer, H., et al.: On the transit Lyα observations of terrestrial planets in the habitable zones of M dwarfs. In preparation, 2018.

EPSC Abstracts
Vol. 12, EPSC2018-830, 2018
European Planetary Science Congress 2018

The search for exoplanetary radio emission: Jupiter as an exoplanet

Jean-Mathias Grießmeier (1,2), Jake D. Turner (3), Philippe Zarka (4,2), Iaroslavna Iaroslavna (5)
(1) Laboratoire de Physique et Chimie de l'Environment et de l'Espace (LPC2E) Université d'Orléans/CNRS, Orléans, France
(2) Station de Radioastronomie de Nançay, Observatoire de Paris, PSL Research University, CNRS, Univ. Orléans, OSUC, 18330 Nançay, France
(3) Department of Astronomy, University of Virginia, VA, USA
(4) LESIA, Observatoire de Paris, CNRS, PSL, Meudon, France
(5) Institute of Radio Astronomy, National Academy of Sciences of Ukraine, Kharkov, Ukraine

Abstract

In the solar system, the magnetized planets are strong radio emitters, the strongest emission being that generated at Jupiter. Theoretical studies suggest that the radio emission from nearby exoplanets could reach intensity levels 3-6 orders of magnitude higher than Jupiter's emission. Several campaigns have been led to search for this emission, but no confirmed detection has yet been reported. Published upper limits are usually based on the theoretical sensitivity of the radio telescope and do not take into account the sporadic nature of the emission. In this paper, we use the radio emission from Jupiter, scale it down in intensity, and determine at what intensity our detection pipeline can still detect the emission. With this method, we can determine the sensitivity of a given telescope and observation setup for a realistic situation.

1. Introduction

The detection and characterization of exoplanetary magnetic fields would open a new window, allowing a better understand of exoplanets, including their formation and their evolution. For this reason, several methods have been suggested which could potentially detect magnetic fields of extrasolar planets. However, most of these methods are prone to false positive detections. This is not the case for planetary auroral radio emission. Therefore, the detection of exoplanetary radio emission can be considered be one of the few method to unambiguously detect exoplanetary magnetic fields ([2]). Over the past decades, this has sparked a number of observational campaigns (see e.g. [3] for an overview), none of which has achieved a confirmed radio detection yet. In parallel, a number of articles have attempted to estimate the radio flux density that can be expected for different types of exoplanets (starting with [6] and [1]). Indeed, according to most recent estimates, emission frequencies are compatible with the frequencies at which some radio telescopes of latest generation operate, and estimated flux densities are close to the sensitivity of these instruments. In particular, [3] find that the flux densities of 15 exoplanets are above the theoretical detection limit of LOFAR as given by [4]. With such encouraging radio predictions, radio observations of exoplanets are undertaken by most low-frequency radio telescopes.

2. Method

In this work, we concentrate on beam-formed observations using LOFAR (the Low-Frequency Array) in the LBA band ($\leq$ 90 MHz). These observations have the advantage of a high time resolution, which can be used to localize and excise short and sporadic RFI precisely. They cannot reliably detect continuous or slowly varying emission, but excel at the detection of short bursty signals. In order to differentiate a physical signal from RFI, we use one ON-beam and two OFF-beams ([4]).

We record radio emission from Jupiter (the ON beam), scale it down in intensity and add it one of the OFF beams. This combined beam ("Jupiter beam") is then compared to the second OFF beam ("OFF-Beam 2"). After RFI cleaning and data reduction (using the pipeline described by [4]), we produce a set of observables which allow to search for exoplanetary radio emission (see Fig. 1 for an example).

We determine by how much we can attenuate Jupiter's signal before the detection pipeline does not detect any statistically significant difference between the "Jupiter beam" and the "OFF-Beam 2". In this way, we can measure the effective sensitivity limit for

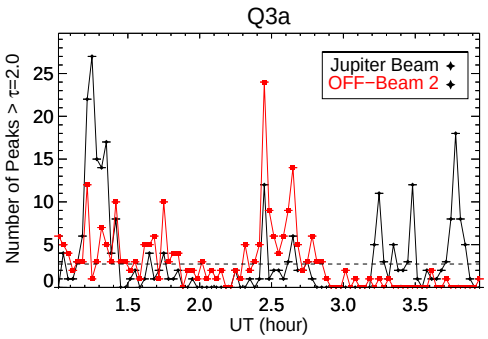

Figure 1: Number of radio emission peaks, compared between the ON-beam (Jupiter) and OFF-beam (observable quantity "Q3a"). Jupiter's emission is mainly localized between 1.2–1.4 UT and 3.2–3.9 UT, whereas the bright emission between 2.3–2.8 UT can be seen in the ON and the OFF beam simultaneously.

a given observational setup.

3. Result

Applied to LOFAR beam-formed observations, we find that radio bursts from a planet at 5 pc could be detected if the flux is 10^6 times stronger than the typical level of Jupiter's radio bursts during active emission events. Equivalently, planets at a distance of 20 pc can be detected assuming the level of emission is 10^6 times stronger than the peak flux of Jupiter's decametric burst emission. This can probably still be improved by future modifications of our detection pipeline.

4. Summary and Conclusions

Usually, published upper limits on exoplanetary radio emission are based on the theoretical sensitivity of a radio telescope, and do not take into account the sporadic nature of the emission. In this paper, we describe a method how to derive upper limits for a realistic situation and apply it to the case of beam-formed observations with LOFAR. We observe Jupiter, divide its signal by a fixed factor before adding it to an observation of "sky background", thereby creating an artificial dataset best described as "Jupiter as an exoplanet". We then run our data processing and signal detection pipeline and check whether the (attenuated) radio signal from Jupiter is detected. The maximum factor by which we can divide Jupiter's signal and still achieve a detection gives the sensitivity of our setup (i.e. the combination of the telescope and the processing chain).

References

[1] Farrell, W. M. and Desch, M. D. and Zarka, P.: On the possibility of coherent cyclotron emission from extrasolar planets, JGR 104, 14025,1999.

[2] Grießmeier, J.-M.: Detection Methods and Relevance of Exoplanetary Magnetic Fields, in Characterizing Stellar and Exoplanetary Environments, Astrophysics and Space Science Library, Vol. 411, Eds. Lammer, H. and Khodachenko, M., Springer, p. 213-237, 2015.

[3] Grießmeier, J.-M.: The search for radio emission from giant exoplanets, in Planetary Radio Emissions VIII, Eds. G. Fischer, G. Mann, M. Panchenko, and P. Zarka, Austrian Academy of Sciences Press, Vienna, p. 285-299, in press, astro-ph 1710.04997, 2018.

[4] Turner, J. D., Grießmeier, J.-M., Zarka, P., Vasylieva., I.: The search for radio emission from exoplanets using LOFAR low-frequency beam-formed observations: Data pipeline and preliminary results for the 55 Cnc system, in Planetary Radio Emissions VIII, Eds. G. Fischer, G. Mann, M. Panchenko, and P. Zarka, Austrian Academy of Sciences Press, Vienna, p. 301-313, in press, astro-ph 1710.04997, 2018.

[5] Turner, J. D., Grießmeier, J.-M., Zarka, P., Vasylieva., I.: The search for radio emission from exoplanets using LOFAR beam-formed observations: Jupiter as an exoplanet, Astronomy and Astrophysics, submitted.

[6] Zarka, P., Queinnec, J., Ryabov, B. P., Ryabov, V. B., Shevchenka, V. A., Arkhipov, A. V., Rucker, H. O., Denis, L., Gerbault, A., Dierich, P., Rosolen, C.: Ground-Based High Sensitivity Radio Astronomy at Decameter Wavelengths, in Planetary Radio Emissions IV, Eds. Rucker, H. O. and Bauer, S. J. and Lecacheux, A., Austrian Academy of Sciences Press, Vienna, 101, 1997.

EPSC Abstracts
Vol. 12, EPSC2018-989, 2018
European Planetary Science Congress 2018

Planetary Magnetism as a Parameter in Exoplanet Habitability

Sarah R.N. McIntyre

Research School of Astronomy and Astrophysics, Australian National University, Canberra, Australia
(sarah.mcintyre@anu.edu.au)

Abstract

Here, we investigate the hypothesis that planetary magnetism has a significant effect on the maintenance of liquid water on an exoplanet by determining which of the currently detected planets have sufficient magnetosphere protection from cosmic and stellar irradiation. We used Olsen & Christiensen's model [1] to determine the maximum magnetic dipole moment of terrestrial exoplanets, further analyzing those located in the Circumstellar Habitable Zone (CHZ). Our results indicate that 70% of exoplanets currently defined as potentially habitable (rocky planets located in the CHZ), even with the best-case scenario of modelling the maximum possible dipole moment with the lowered magnetic protection threshold value of $0.55M_{\oplus}$, would not have a magnetic field strong enough to protect their surface, and consequently any potential water or life on it, against stellar and cosmic irradiation.

1. Introduction

Within the next decade upcoming observations with near-future telescopes, will provide us with ever-increasing number of planets. In order to make the most of the limited observational resources available, optimal target selection will be of the utmost importance. Selection of targets currently relies on "classically" defined habitable zone, constrained only by the density of the planet and the distance from its host star. More than ever it is important to expand to a multi-parameter approach and include factors such as magnetic field, albedo, tidal locking, impact events, and plate tectonics. This multi-parameter approach to habitability (M-PAtH) will enable us to rank the current habitable worlds and provide a justified priority of those most likely to maintain liquid water (and host life) in order to best utilize telescope time when biosignature observations become a possibility.

The majority of our assessments on habitability stems from what we have observed in our own solar system. One of the differences between Earth and Mars/Venus is the presence of a strong magnetic dipole moment that protects the surface and is hypothesized to shield surface liquid water from solar winds and flares [2]. Venus, Earth and Mars likely began with similar amounts of water since they are all about the same size and formed at the same time (~4.5 billion years ago) [3]. This is corroborated by their Deuterium to Hydrogen ratios (D/H) displayed in Table 1 which suggests that both Mars and Venus had more water early in their histories. Yet today, only Earth has managed to retain most of its water.

Table 1: Atmospheric loss and isotope ratios

Planet	D/H ratio ($\times 10^{-4}$)
Venus	160 ± 20
Earth	1.49 ± 0.03
Mars	9.24 ± 1.66

In the absence of sufficient magnetic protection, the upper atmosphere of an exoplanet will be directly exposed to stellar winds and coronal mass ejections, resulting in atmospheric mass-loss due to non-thermal processes such as ion pickup, photo-chemical energizing mechanisms, and sputtering [4]. Since, planetary magnetism and the parameters of stellar plasma flows (including speed and density) are important methods of non-thermal atmospheric erosion, these factors could affect the evolution of a planet's environment and its potential habitability [5]. Here we focus on modelling the magnetic dipole moment of detected terrestrial exoplanets to determine their strength and consequent ability to protect their atmospheres from stellar effects.

2. Magnetism Model

Olson & Christiensen's [1] magnetic moment scaling law is currently the best available model and has been utilised in our calculations:

$$M = 4\pi r_0^3 \gamma \left(\frac{\bar{\rho}_0}{\mu_0}\right)^{1/2} (FD)^{1/3} \quad (1)$$

where M is the magnetic dipole moment (in Am^2), γ is a fitting coefficient with a value of 0.1 – 0.2 deduced from numerical simulations [1], $\bar{\rho}_0$ is the bulk density of the fluid in the outer liquid core, which we have modelled based on Earth's density models ($\bar{\rho}_0 = 11\times10^6\ gm^{-3}$), μ_0 is the magnetic permeability of the vacuum ($\mu_0 = 4\pi\times10^{-7} H/m$), and D is the thickness of the outer liquid core rotating shell where convection occurs, modelled as $0.65r_o$ according to Heimpel et al. [6]. The planetary core radius parameter (r_o) was calculated using Zeng et al.'s semi-empirical relationship between core radius fraction, planetary radius, and mass for rocky planets [7][8]. The final factor in equation 1 is the average convective buoyancy flux, F, and we have used Lopez-Morales et al.'s equation to model this parameter [9]:

$$\frac{F}{F_\oplus} = \left(\frac{R_{O_l}}{R_{O_{l\oplus}}}\right)^2 \left(\frac{D}{D_\oplus}\right)^{2/3} \left(\frac{\Omega}{\Omega_\oplus}\right)^{7/3} \quad (2)$$

where the local Rossby number (R_{O_l}= 0.1) gives F_{max}, which, in turn allows us to estimate the maximum dipolar magnetic moment. Since we do not have the planetary rotation rates (Ω) for all the currently detected terrestrial exoplanets, we examined the rotation periods of 70 solar system objects including planets, dwarf planets, their moons, Kuiper belt objects and main-belt asteroids to estimate an average rotation rate of $\sim 1.52 \pm 0.36\ \Omega_\oplus$. Additionally, Grießmeier et al. was used to determine which exoplanets were tidally locked, as their orbital period will be equal to their rotation period [10]. These two rotation rate scenarios were used in calculations of equation 2.

3. Results

The maximum magnetic dipole moments of all confirmed terrestrial exoplanets were modelled and a clear trend between M and r_o was observed (Figure 1).

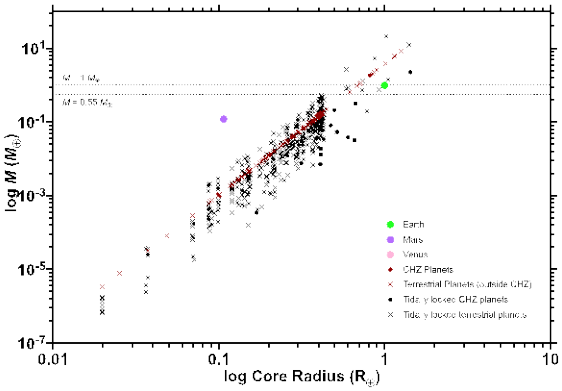

Figure 1: Maximum dipolar magnetic moments as a function of planetary core radius for both angular momentum scenarios: $1.52\Omega_\oplus$ (red), Tidally locked (black). Dotted lines signify magnetic moment threshold values.

It has been hypothesized that planets with a magnetic dipole moment of equal or greater strength than Earth's would have a magnetic field strong enough to protect the surface of the planet and preserve liquid water [9]. Therefore, we have set a threshold value of $1M_\oplus$ to determine which exoplanets could be classified as "magnetically habitable" i.e. protects surface water/life. Figure 1 shows that amongst our current sample, not all exoplanets possess a strong magnetic dipole moment. In spite of the fact that we modelled the best case scenario by calculating the maximum possible magnetic dipole moment, out of the 735 terrestrial planets in our model, only 21 of them had a magnetic moment equal to or larger than that of Earth's. However, would a lower magnetic moment value still adequately protect the surface of an exoplanet?

To answer this question, we once again looked to Earth, but instead of its current features, we examined the evolution of Earth's magnetic dipole moment. Based on models of mantle cooling from Tarduno et al., the paleointensity data suggests a virtual dipole moment of 3.8 (±0.4) x 10^{22} Am^2 for the NGB dacite ~3.45 Gya [11]. Since water and life were present on Earth at this time, we can reduce our lower limit on the magnetic dipole moment parameter from $\geq 1M_\oplus$ to $\geq 0.55M_\oplus$.

To determine the effect of planetary magnetism on terrestrial exoplanets in and near the circumstellar habitable zone (CHZ), we examined the maximum magnetic dipole moment values in the context of the optimistic and conservative habitable zones. Figure 2

showcases the probability of the CHZ exoplanets' magnetic moment being $\geq 0.55M_{\oplus}$. Probability values greater than 50% indicate a high likelihood that the planet has a magnetic moment strong enough to be classified as magnetically habitable; however, all exoplanets that have a non-zero probability of being $\geq 0.55M_{\oplus}$ are labelled as there is a chance that the planet has a magnetic moment strong enough to be protect the surface from stellar radiation.

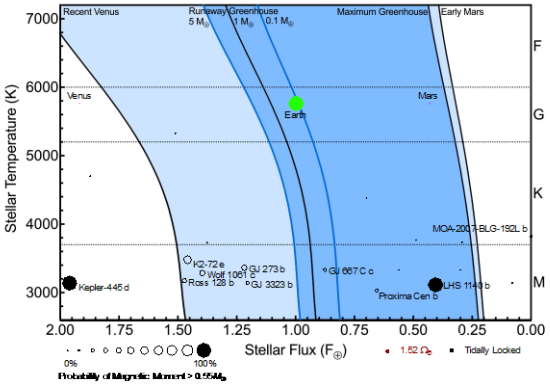

Figure 2: Sample of potentially habitable terrestrial planets and their location within the CHZ [8][9]. Size and opacity indicate the planets probability of having a magnetic moment strong enough to protect the surface of the planet from stellar effects. The planets that are labelled have a non-zero probability of having a magnetic moment $\geq 0.55M_{\oplus}$.

4. Summary and Conclusions

The results of the modelling and analysis revealed that a large number of planets currently defined as potentially habitable (rocky planets located in the CHZ), even with the best-case scenario of modelling the maximum possible dipole moment with the lowered threshold value, would not have a magnetic field strong enough to protect their surface, and any potential water or life on it, against stellar and cosmic irradiation. Based on our results of planetary magnetism and HZ boundaries, there are 4 exoplanets that consistently showed a significant magnetic protection: - K2-72 e, LHS 1140 b, GJ 273 b and Wolf 1061 c. Furthermore, Proxima Cen b, Trappist 1f and Trappist 1d show ~20% chance of having a strong enough magnetic field to protect their surfaces once the threshols is lowered, so there is a chance that they could be magnetically habitable.

Perhaps the most interesting outcome of Figure 2 is the effect that the magnetic moment value of Kepler-445 d could potentially have on definition of habitability. It could provide the opportunity to re-examine some of the "inhabitable" planets such as Kepler-445 d which, due to as yet unexplored circumstance, could potentially support liquid water in parts of their environment. If the habitable zone concept is based on the amount of incident stellar flux that reaches the surface of a planet so as to provide a planetary temperature suitable for liquid water, would it be possible that Kepler-445 d, which, despite being closer to its host star than the conventional HZ would allow, but due to having a magnetosphere 6 times as strong as Earth's, could be protected from the stellar rays and winds enough to provide a planetary surface environment suitable for liquid water?

While the models utilised here provide a broad overview of planetary magnetism, they do not account for changes of F and D with age, or for the effect of extreme external conditions, such as e.g. highly inhomogeneous heating or very strong stellar winds. More research on the star planet magnetic interactions needs to be done to determine how much effect the different stellar types and ages have on their planetary companions. Future research on this could more accurately inform the threshold limits for various stellar scenarios.

Our results showcase that introducing planetary magnetism as a parameter in habitability calculations in conjunction with the CHZ, limits the list of potentially life bearing exoplanets and provides more information on where we should begin our observational measurements. There are many more factors that we need to consider in order to further reduce the potential thousands of Earth-like planets to be discovered in the near-future using instruments such as TESS and CHEOPS. Examining the significance of planetary magnetism is the start of combining the current knowledge of astronomical and planetary features to narrow down our search for life and give our future observations the best possible starting point.

Acknowledgements

Thanks go to Charley Lineweaver, Michael Ireland, and Mark Krumholz for helpful discussions, comments and correspondence. S.R.N.M gratefully acknowledges an Australian Research Council Research Training Program scholarship.

References

[1] Olson, P., and Christensen, U. R.: Dipole moment scaling for convection-driven planetary dynamos, Earth and Planetary Science Letters, Vol. 250(3-4), pp. 561-571, 2006.

[2] Elkins‐Tanton, L.: What makes a habitable planet?, Eos, Transactions American Geophysical Union, Vol. 94(16), pp. 149-150, 2013.

[3] Grinspoon, D. H.: Implications of the high D/H ratio for the sources of water in Venus' atmosphere, Nature, Vol. 363(6428), pp. 428, 1993.

[4] Vidotto, A. A.: The effects of stellar winds and magnetic fields on exoplanets, Proceedings of the International Astronomical Union, Vol. 9(S302), pp. 228-236, 2013.

[5] Güdel, M., Dvorak, R., Erkaev, N., Kasting, J., Khodachenko, M., Lammer, H., ... and Wood, B. E.: Astrophysical conditions for planetary habitability, arXiv preprint arXiv:1407.8174, 2014.

[6] Heimpel, M., Aurnou, J., and Wicht, J.: Simulation of equatorial and high-latitude jets on Jupiter in a deep convection model, Nature, Vol. 438(7065), pp. 193, 2005.

[7] Zeng, L., Sasselov, D. D., and Jacobsen, S. B.: Mass–radius relation for rocky planets based on PREM. The Astrophysical Journal, Vol. 819(2), pp. 127, 2016.

[8] Zeng, L., and Jacobsen, S. B.: A Simple Analytical Model for Rocky Planet Interiors, The Astrophysical Journal, Vol. 837(2), pp. 164, 2017.

[9] López-Morales, M., Gómez-Pérez, N., and Ruedas, T.: Magnetic Fields in Earth-like Exoplanets and Implications for Habitability around M-dwarfs, Origins of Life and Evolution of Biospheres, Vol. 41(6), pp. 533-537, 2011.

[10] Grießmeier, J. M., Stadelmann, A., Grenfell, J. L., Lammer, H., and Motschmann, U.: On the protection of extrasolar Earth-like planets around K/M stars against galactic cosmic rays, Icarus, Vol. 199(2), pp. 526-535, 2009.

[11] Tarduno, J. A., Cottrell, R. D., Watkeys, M. K., Hofmann, A., Doubrovine, P. V., Mamajek, E. E., ... and Usui, Y.: Geodynamo, solar wind, and magnetopause 3.4 to 3.45 billion years ago, Science, Vol. 327(5970), pp. 1238-1240, 2010.

EPSC Abstracts
Vol. 12, EPSC2018-1054, 2018
European Planetary Science Congress 2018

The Kompot Code: first-principles upper atmosphere modelling and the evolution of planetary atmospheres

Colin P. Johnstone
University of Vienna, Department of Astrophysics, Türkenschanzstrasse 17, 1180 Vienna, Austria

Abstract

Understanding the physical structures of planetary atmospheres under a variety of conditions is necessary for understanding atmospheric evolution and the roles of escape to space. We present here The Kompot Code, which calculates the thermal, chemical, and hydrodynamic structures of planetary atmospheres for arbitrary conditions. The model is 1D and attempts to take into account all of the major physical processes that influence the structure of the atmosphere. We demonstrate how this model can be applied to a range of planets with different atmospheric compositions and inputs from the central star.

1. Introduction

The physical properties of a planet's upper atmosphere are crucially dependent on a large number of factors. These include the planet's mass, the chemical composition of the atmosphere, the planet's orbital distance from the central star, and the magnetic activity level of the star. To properly take into account all of these factors, models that include as many of the relevant physical processes as possible are needed. The most important physical processes include hydrodynamic expansion and contraction of the gas, chemistry, including photoreactions and ion chemistry, diffusion processes such as eddy and molecular diffusion, heating of the gas by stellar X-ray, UV, and IR radiation, and the transport of heat within the atmosphere by conduction and energy exchanges between different components of the gas. Much work is still needed for models that combine such processes in complete and self-consistent ways, both in developing such models and in applying them to a range of planetary cases.

2. The Kompot Code

We have developed The Kompot Code (Johnstone et al. submitted), which applies the physical processes listed above to planets with arbitrary properties. In all cases, we have attempted to model these processes from first-principles physical considerations, as much as is practical, though much improvement to the model is planned for future work. The model is 1D and and extends from some altitude in the middle atmosphere to the exobase, as shown in Fig. 1. We have validated our model by applying it to the cases of modern Earth and Venus and found good agreement for both the thermal and chemical structures.

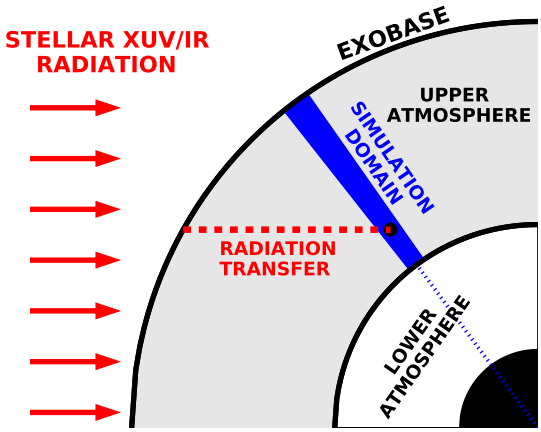

Figure 1: Figure showing the computational domain calculated by The Kompot Code. The domain extends from an arbitrary location in the middle atmosphere to the exobase and can be at any angle relative to the incoming radiation.

The code models the gas as three components, i.e. neutrals, ions, and electrons, with their own separate temperatures. The chemical network used contains 63 species, including 30 ion species, and 503 reactions, including 56 photoreactions and 7 reactions involving impacts with non-thermal photoelectrons. The two stellar inputs are the XUV (i.e. X-ray and ultraviolet)

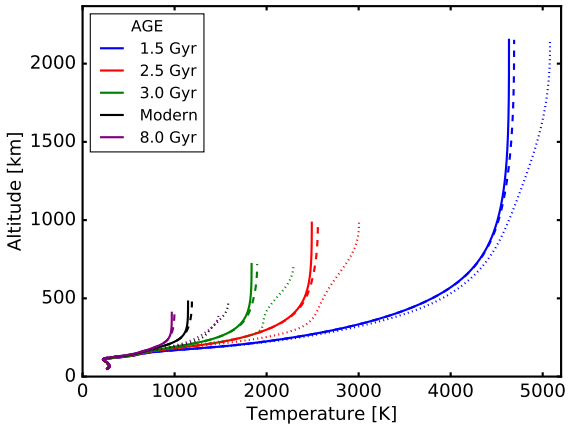

Figure 2: Figure showing the structure of the Earth's upper atmosphere at different ages from Johnstone et al. (submitted). In all cases, the lower atmospheric properties are assumed to be equal to those of the modern Earth and the only difference has been the input XUV spectrum of the Sun.

field between 1 and 400 nm, and the IR field between 1 and 20 μm. In addition, we calculate the spectrum of non-thermal photoelectrons created by photoionisation reactions. The heating of the gas takes place due to a range of processes: these are direct heating by the absorption of stellar XUV radiation, heating from exothermic chemical reactions, electron heating from elastic collisions with non-thermal electrons, heating by the absorption of stellar IR radiation, and Joule heating. The gas is cooled by IR emission from several molecules: these are CO_2, NO, O, H_2O, and H_3^+. Thermal conduction is calculated for the neutral, ion, and electron components separately, and the energy exchanges between these components are also calculated.

3. Discussion

Our model can be applied to a large range of systems. As an example, we show calculations for the upper atmosphere of the Earth at different ages between approximately 3 Gyr in the past to approximately 2.5 Gyr in the future. In all cases, the simulations differ from our model of the modern Earth only in the input solar XUV spectrum. At younger ages, the Sun was more active in X-rays and UV wavelengths than it currently is, and so the atmosphere was hotter and more extended. This likely has significant effects on atmospheric losses during these times. We plan to apply this code to better understand both the atmospheric evolutions of our own solar system planets and the formation of atmospheres on planets in a exoplanet systems.

Acknowledgements

This study was carried out with the support by the FWF NFN project S11601-N16 "Pathways to Habitability: From Disk to Active Stars, Planets and Life" and the related subprojects S11604-N16, and S11607-N16.

References

[1] Johnstone, C. P., M. Güdel, H. Lammer, and K. G. Kislyakova (2018), The Upper Atmospheres of Terrestrial Planets: Carbon Dioxide Cooling and the Earth's Thermospheric Evolution, submitted to Astronomy & Astrophysics.

EPSC Abstracts
Vol. 12, EPSC2018-1078, 2018
European Planetary Science Congress 2018

Sub-Alfvenic magnetosphere of a Hot Jupiter

Alexander Lavrukhin, David Parunakian and Igor Alexeev
Skobeltsyn Institute of Nuclear Physics M.V.Lomonosov Moscow State University, Moscow, Russia

Abstract

In this work we investigate properties of Hot Jupiter class exoplanet magnetospheres in cases where the relative velocity of a planet and the stellar plasma flow around it is sub-Alfvenic (i.e. the vector sum of the plasma flow velocity and the exoplanet orbital velocity is less than the local Alfven velocity). Under these conditions a special current structure known as Alfven wings develops in the magnetosphere.

1. Introduction

Alfven wings connect an exoplanet's ionosphere and magnetosphere with the chromosphere of the host star. In this case the exoplanetary magnetosphere structure depends entirely on the structure of the Alfven wings.

Most known exoplanets are located in orbits closer than 0.6 AU, which leads to intense heating, ionization, and chemical changes in the upper atmosphere induced by stellar radiation. This leads to expansion of ionized atmospheric material, which can then form an equatorial plasma disk in the exoplanetary magnetosphere.

2. Summary and Conclusions

In our work we consider possible physical conditions in a typical Hot Jupiter orbit and examine the structure of a magnetosphere with Alfven wings, both with and without a plasma disk.

EPSC Abstracts
Vol. 12, EPSC2018-1134, 2018
European Planetary Science Congress 2018

Alfvenic current system in Saturn's magnetosphere and time variation of the magnetic field in the outer Saturn magnetosphere.

Igor I. Alekseev (1), Elena S. Belenkaya (1), Stan W.H. Cowley (2), Aleksander S. Lavrukhin (1), David A. Parunakian (1), Ivan A. Pensionerov (1)
(1) Federal State Budget Educational Institution of Higher Education M.V. Lomonosov Moscow State University, Skobeltsyn Institute of Nuclear Physics (SINP MSU), 1(2), Leninskie gory, GSP-1, Moscow, 119991, Russian Federation;

(2) Department of Physics & Astronomy, University of Leicester, Leicester LE1 7RH, UK. (alexeev@dec1.sinp.msu.ru)

1. Introduction

As pointed out in particularly by Cowley et al. [1], the magnetosphere-ionosphere interactions in the case of rapidly rotated planets with additional source of inter-magnetospheric plasma, results that the magnetospheric plasma cannot state in the rigid corotation together with the planet. Slipping of the magnetospheric plasma relative to the outer atmosphere results in the generation of the equatorial plasma magnetodisk with embedded strong thin azimuthal currents. The same process results in the generation of potential drop along the magnetic field lines, as well as the electrons beams acceleration and powerful aurora emitting by the upper atmosphere. The very high field-aligned conductivity requires that magnetic field lines be equipotential (parallel electric field must be zero) and angular velocity must be the same at the ionosphere and in the equatorial plane, but beyond the Alfvenic radius magnetic field can not control of the plasma flow in the magnetosphere, and specific 3D current system will be generated.

2. Ionospheric and field-aligned currents.

We describe all toroidal and poloidal currents connected by each to other through the ratio of the Pedersen and Hall ionospheric conductivities as parts of the total current system. We added the azimuthal field B_phi created by the field-aligned currents to the global paraboloid model of the magnetic field in the Kronian magnetospheres [2]. Because the ionospheric part of the total current loop controlled by ionospheric conductivity, and the conductivity is determined by precipitation electron flux, we have a positive feedback. The electron beams results in increasing of Hall conductivity and last effect increase the field-aligned potential drop and the energy exchange between neutral atmosphere

Acknowledgements

I. Alexeev, M. Khodachenko, E. Belenkaya A. Lavruchin, D. Parunakian, and I. Pensionerov acknowledge the support of the Ministry of Education and Science of the Russian Federation Grant RFMEFI61617X0084.

References

[1] Cowley, S. W. H., I. I. Alexeev, E. S. Belenkaya, E. J. Bunce, C. E. Cottis, V. V. Kalegaev, J. D. Nichols, R. Prangé, and F. J. Wilson, A simple axisymmetric model of magnetosphere-ionosphere coupling currents in Jupiter's polar ionosphere, J. Geophys. Res., 110, A11209, doi:10.1029/2005JA011237. 2005.

[2] Alexeev I. I., Belenkaya E. S. Modeling of the Jovian Magnetosphere // Annales Geophysicae. V. 23. No. 3. P. 809-826. 2005.